Gravitational Reference Sensor Technology Development Roadmap for the Mass Change Mission

4 May 2020

Lead Author: John W. Conklin
jwconklin@ufl.edu, University of Florida, Mechanical and Aerospace Engineering Department, MAE-A 322, Gainesville, FL 32611

Co-Authors: Peter Wass[1], Pep Sanjuan[1], Guido Mueller[1], John Ziemer[2], Brent Ware[2], James Leitch[3], Jennifer Lee[3]
[1]University of Florida, [2]California Institute of Technology / Jet Propulsion Laboratory, [3]Ball Aerospace

Abstract: Low-low satellite-to-satellite tracking missions like GRACE-FO that utilize laser ranging intereferometers are technologically limited by the acceleration noise performance of the electrostatic accelerometers, in addition to temporal aliasing issues associated with the dynamic gravity field measurements. The current accelerometers, used in the GRACE and GRACE-FO mission have a limited sensitivity of ~10^{-10} m/s^{2}Hz$^{1/2}$ around 1 mHz. Meanwhile, the LISA Pathfinder mission, which was a technology demonstrator for the future ESA/NASA LISA gravitational wave mission, demonstrated an acceleration noise performance of 2×10^{-15} m/s^{2}Hz$^{1/2}$ around 1 mHz. The results of LISA Pathfinder and extensive ground testing using precision torsion pendula indicate that a simplified version of the LISA Pathfinder gravitational reference sensor (GRS) could be used in future Earth geodesy missions beyond GRACE-FO. Such a sensor would have an acceleration noise below 10^{-12} m/s^{2}Hz$^{1/2}$, which is understood to be the desired performance for future Earth geodesy missions utilizing laser interferometry for intersatellite ranging. This sensor could be directly integrated with the laser interferometer, potentially relaxing requirements on spacecraft attitude measurement and control, or it could be operated as a stand-alone instrument with a stable structural reference to the laser interferometer reference point. The improved performance is enabled by increasing the mass of the sensor's test mass, increasing the gap between the test mass and its electrode housing, removing the small grounding wire used in the GRACE accelerometers and replacing them with a UV LED-based charge management system. The sensor's performance would be optimized on a drag-compensated platform but could also operate on a traditional spacecraft utilizing control schemes tailored to the specific spacecraft platform with reduced performance. Here, we describe a GRS optimized for mass change missions, as well as a technology development effort needed to bring the instrument to TRL 6. We assume that this sensor would initially be implemented as a technology demonstration on a non-drag-free GRACE-like satellite, but could later be implemented on a drag-free platform. We therefore present the GRS's performance under both scenarios. The instrument would have a volume of ~10^4 cm^3, a mass of ~15 kg, and a nominal power consumption of ~20 W per spacecraft. Development of this instrument to TRL 6 for incorporation as a technology demonstration on the next Mass Change Mission would require ~4 years of effort, and the delivery of flight units could be completed ~2 years later. Finally, it is important to note that *LISA Pathfinder has demonstrated that the GRS architecture has no technical barriers to achieving even orders of magnitude better performance in the future*. Thus, investment in the development of this technology opens up a path to continued mass change sensitivity improvements that could be pursued in parallel with laser ranging and other vital technology advancements.

1 Description of the Technology and its Benefits

1.1 *Benefits of Improved Acceleration Noise*

The utility of the GRACE and GRACE-FO data have been substantial for climate-related research. Several studies have focused on understanding the full error budget of the GRACE and GRACE-FO missions, as well as how to lower the error levels for future missions. The gravity field retrieval errors fall into two categories: measurement system errors due to the performance of the onboard measurement system (the inter-satellite ranging instrument and accelerometer for GRACE-FO), and temporal aliasing errors due to undersampling of high frequency mass variations in the Earth system such as ocean tides and weather systems. Temporal aliasing errors are currently the largest source of error limiting the spatial resolution of the gravity fields (Figure 1). If the error associated with temporal aliasing can be reduced by either increasing the number of spacecraft employed or improving temporal aliasing models, then the gravity field retrieval becomes dominated by measurement system errors, the largest of which is the accelerometer (Figure 1). Hence, there is a need to improve upon the performance of the current electrostatic accelerometers flown on GRACE-FO. The simplified gravitational reference sensor (GRS) described here provides the same function as the GRACE accelerometers, but with at least a factor of 100 improved acceleration noise performance. It takes advantage of the flight heritage of LISA Pathfinder, which demonstrated a 10^5 improvement over GRACE-FO and ~10^3 improvement over GOCE (Armano, et al., 2018).

1.2 *The LISA Pathfinder Gravitational Reference Sensor*

The state of the art in ultra-precise inertial sensors (or accelerometers) is the LISA Pathfinder inertial sensor, shown in Figure 2. It uses a 2 kg, Au/Pt test mass (TM) inside a molybdenum electrode housing (EH). The housing contains 12 gold coated electrodes to differentially sense the position and orientation of the cube via capacitive sensing and to actuate it using electrostatic actuation. Six "injection electrodes" are driven with a 100 kHz AC bias voltage to frequency shift the capacitive measurement to high frequency. Readout of the sensing electrodes and driving of the actuation electrodes is performed by the front end electronics (FEE). The gap between the TM and housing is 4 mm and is a trade-off between reducing the effects of noise sources, e.g. from uncontrolled potentials on the electrodes, and being able to measure test mass displacement at the

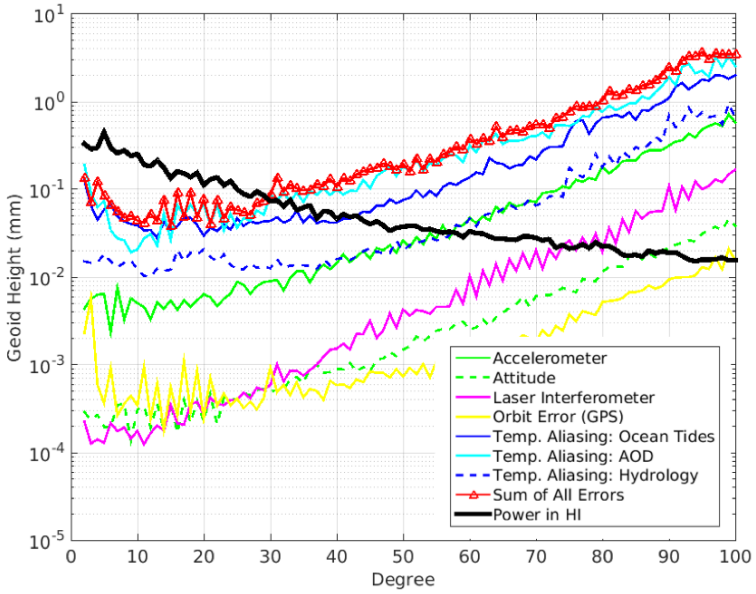

Figure 1. Geoid height error for a simulated mission of a single pair of satellites at 500 km altitude. Shown is the impact of each individual source of error on the gravity retrieval. The black curve is the power in the hydrology and ice signal that we wish to recover. It is seen that the largest source of error on the gravity field recovery is due to temporal aliasing errors. The largest measurement system error is from the accelerometer.

nanometer level over the measurement bandwidth. The capacitive readout system is arranged such that electrodes facing opposing faces of the test mass are combined via a capacitive bridge. A change in the position of the test mass gives a differential, bi-polar, signal at the output of the bridge, which is used as an input to the drag-free control system. A caging and venting mechanism (CVM) uses a set of mechanical fingers to secure the TM during launch (Bortoluzzi, Conklin, et al., 2013). During science operations, the TM charge is controlled by a charge management system (CMS) based on UV photoemission using Hg vapor lamps as the UV light source (Wass, et al., 2018). The CMS eliminates the need for the small grounding wire used in the ONERA accelerometers that both limits their performance and potentially causes challenges during integration and test.

LISA Pathfinder, launched in December of 2015, exceeded all expectations in terms of acceleration noise performance. Acceleration noise is caused by residual spurious forces acting on the TM, and it is the primary metric used to evaluate the performance of these instruments, as well as accelerometers. The goal of the LISA Pathfinder mission was to demonstrate a differential acceleration noise level between the two LISA Pathfinder test masses of 3×10^{-14} m/s^{2}Hz$^{1/2}$ above 1 mHz, the same frequency band that is important for Earth geodesy. Figure 3 shows the final results from the LISA Pathfinder mission, which exceeded its requirements by more than an order of magnitude. At 1 mHz the measured performance was 2×10^{-15} m/s^{2}Hz$^{1/2}$, more than a factor of 10^4 over the performance of GRACE and GRACE-FO and 10^3 over that of GOCE.

1.3 *A Simplified Gravitational Reference Sensor for Earth Geodesy*

The acceleration noise performance of inertial sensors, like that of LISA pathfinder, scales linearly with the mass of the test mass and at least linearly with the gap size between the test mass and the electrode housing. The results of LISA Pathfinder show that a similar, but scaled-down design could achieve $\leq10^{-12}$ m/s^{2}Hz$^{1/2}$ for example with a TM on the order of a few 100 g and an electrode housing on the order of $5\times5\times5$ cm^3. The lower TM mass in turn enables a simplified caging mechanism.

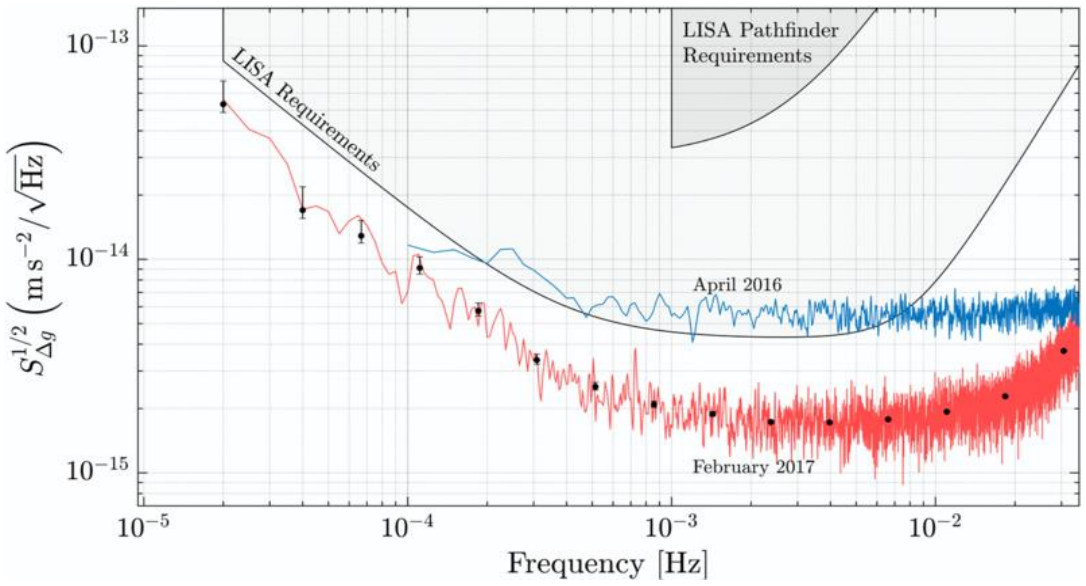

Figure 3. Measured LISA Pathfinder acceleration noise performance and the requirements for the LISA gravitational wave observatory (Armano et al., 2018). The frequency band of interest for LISA is the same as that for Earth geodesy.

The key improvements of this simplified GRS over the accelerometers flown on GRACE and GRACE-FO are the following.

1. *Increase TM-to-electrode housing gap size to ~1 mm and increase TM mass to 250-500 g*
   These two key design parameters enable better acceleration noise performance by reducing the TM acceleration associated with several critical TM surface force noise contributions (see Box 1).
2. *Remove the small TM grounding wire and replace it with UV LED charge control*
   The thermal noise associated with the grounding wire limits the acceleration noise of the GRACE accelerometers to ~10^{-11} m/s^{2}Hz$^{1/2}$ around 1 mHz (Lebat et al., 2013). Eliminating this wire would (a) remove this performance limitation, (b) allow larger TM-EH gap sizes to be used, and (c) mitigate challenges associated with installing this wire during assembly, integration and test. In place of a grounding wire, a UV photoemmsion-based charge control would be employed. This technology was first demonstrated by Gravity Probe B and more recently by LISA Pathfinder.
3. *Reduce the impact of environmental factors on the sensor's performance*
   Key to the performance of inertial sensors is isolating the test mass from its host platform. Larger gaps between the test mass and spacecraft and removal of the grounding wire are important for improving this isolation. We also plan to vent the volume around the test mass to space to reduce the residual pressure around the test mass. This reduces several dominant acceleration noise sources, including Brownian noise and those arising from temperature gradient fluctuations. Magnetic shielding may also be employed to reduce forces caused by the Earth's magnetic field and fields generated by the spacecraft.
4. *Operate the sensor on a drag-free or drag-compensated spacecraft*
   Test mass electrostatic actuation noise is one of the leading acceleration noise sources for traditional electrostatic accelerometers. If the GRS were operated on a drag-compensated platform, then the required actuation force could be reduced to zero (drag-free) or near zero (drag-compensated), thus simultaneously reducing the actuation noise to near-zero. If operated on a traditional spacecraft, like GRACE or GRACE-FO, then test mass actuation force would dominate the noise budget of the GRS (see Section 1.5), reducing its acceleration noise performance by about a factor of ten, which would still represent a ten-fold improvement over the GRACE accelerometers.

1.3.1 GRS Test Mass and Electrode Housing

The flight-proven configuration of the LISA Pathfinder TM and electrode housing, described in Section 1.2, is envisioned to be used in the simplified GRS. We expect a cubic test mass, ~30 mm in length, constructed from a high density metal with low magnetic susceptibility. The AuPt alloy used in LISA Pathfinder is a strong candidate due to its high density (20 g/cm^3). An alternate, BeCu, has a susceptibility that is a factor of ten lower than that of AuPt, reducing requirements on the spacecraft magnetic environment, although its density is half that of AuPt, increasing the acceleration noise associated with all surface forces (see Section 1.4).

The EH electrode geometry would be similar to that of LISA Pathfinder, but could be modified to reduce TM translational and rotational coupling along the sensitive direction, aligned with the laser interferometer (Conklin, 2015). The overall size of the EH would be scaled according to the TM. It would have ~10 mm thick walls, constructed from either aluminum, with ceramic electrode spacers, which is low mass and has high thermal conductivity, or be constructed from molybdenum

with sapphire spacers, following the LISA Pathfinder design. If molybdenum were used, the EH would have a mass of approximately 1 kg.

1.3.2 Charge Management System

The CMS for the simplified GRS would follow that of the LISA mission, which will employ a UV LED-based charge management system. UV light would delivered to the electrode housing via a fiber optic cable directed toward the interior surface of the EH to produce photoelectrons. Compared to the Hg lamps used in LISA Pathfinder as the UV source, these newer UV LEDs are smaller, lighter, consume less power, and have a higher dynamic range, with at least an order of magnitude improvement in each performance area (Olatunde, et al., 2015). The ability to modulate these UV LEDs quickly, enables a charge control scheme using a single UV LED that continuously maintains the TM near 0 V in a passively (open loop) stable way. In this charge control method, the UV LED output is pulsed synchronously with the AC electric field used for the capacitive readout inside the EH. The phase of the UV light relative to the electric field governs the magnitude and direction of photoelectron flux between the TM and the EH. After an on-orbit calibration process, the phase of the UV light pulses would be set to maintain the TM potential close to zero continuously using extremely low levels of UV power (<1 nW). This charge control method is one of the planed operational modes for LISA, and it has been validated by experiments using the torsion pendulum facility at the University of Florida, described below, as well as a similar apparatus at the University of Trento, Italy.

1.3.3 Integrated Electronics

The GRS electronics, which comprises both analog and digital elements, performs the following functions:

- Digitally generate the test mass injection bias to frequency shift the capacitive readout from low frequency to the injection frequency (e.g. 100 kHz)
- Perform the six degree of freedom position readout of the test mass by differencing opposing pairs of sensing electrodes via analog electronics, and demodulating the differenced signals at the injection frequency via digital electronics
- Apply actuation voltages (digitally) to the sensing electrodes (at DC or audio frequencies) to control the position and orientation of the test mass
- Provide the analog current source for the UV LEDs to discharge the test mass
- Command the caging and positioning mechanism (digital and analog)
- Perform general instrument control, provide telemetry to the spacecraft bus, and handle safe mode conditions (digital)

The digital functions could likely by performed by a single FPGA-based control board, while separate analog electronics boards would be needed for the UV LED current source, the analog portion of the capacitive readout, and power distribution. In total the electronics unit is expected to have a mass ~4 kg and consume ~20 W during nominal operation.

1.3.4 Caging and Positioning Mechanism

The caging and positioning mechanism (CPM) would be a simplified version of the LISA Pathfinder caging and venting mechanism (CVM) and grabbing, positioning and release mechanism (GPRM) combined into a single unit. The CVM on Pathfinder used eight mechanical fingers to hold the TM with kN-level loads to secure it against launch loads. Once on orbit, the CVM retracts, handing the TM over to the GPRM and simultaneously opening a vent port in the GRS vacuum chamber to reduce the pressure in the vicinity of the TM by venting residual gas to space. The GPRM is a low preload mechanical finger that grabs the TM on opposing sides and

releases it into free-fall motion. The GPRM is also capable of re-grabbing the TM mechanically in the event of a safemode on board the spacecraft (Bortoluzzi, Conklin, et al., 2013).

The simplified GRS CPM can be a single, less complicated mechanism for two reasons. First, the TM mass of the simplified sensor is 4-8 times lower than that of the LISA Pathfinder test mass, reducing the force required to constrain it during launch. The second reason is that the in-flight performance of the LISA GPRM has been well characterized, and LISA Pathfinder flight data can be used to develop a simpler mechanism. In particular, data from LISA Pathfinder indicates that adhesive "cold-welding" forces between the GPRM and the test mass are less critical than was thought prior to launch. The CPM envisioned could be a mechanism similar to the LISA Pathfinder GPRM, but with the capability of producing higher preloads on the TM.

1.4 *Acceleration Noise Modeling*

Roughly 30 different noise sources become relevant at acceleration noise levels below 10^{-12} m/s^2 Hz$^{1/2}$ (Gerardi et al., 2014). Generally, noise contributions can be divided in two main classes: bulk interactions and surface interactions. Surface interactions are the most numerous and often dominant, while bulk interactions are generally related to macroscopic quantities such as mass, charge, and magnetic moment. An incomplete list of these interactions is listed in Box 1.

In addition to the numerical models and measured results obtained by LISA Pathfinder science team, torsion pendulum facilities located in Trento, Italy and the University of Florida (Figure 4) have been used to quantify noise sources by measuring excess noise with respect to the thermal noise limit imposed by the suspension fiber. The University of Florida (UF) torsion pendulum facility consists of a 1 m long, 50 μm diameter tungsten fiber, which supports a cross-bar with a test mass at each of the four ends. Each test mass is a thin-walled, hollow aluminum cube, connected by 22 cm-long shafts to a central block (Ciani et al., 2017). These shafts convert the

Box 1: Test Mass Surface and Bulk Interactions

- *Thermal gradient fluctuations*: Differences in the finite temperature of the housing induce forces on the TM via differential outgassing and the radiometer effect (Carbone et al., 2007).
- *Residual gas damping*: Brownian noise from residual gas trapped in the gaps around the TM. This effect is amplified in a constrained volumes like accelerometers (Cavalleri et al., 2009).
- *Stray DC voltages and TM charge*: The interaction of stray voltages of 10-100 mV (Carbone et al., 2005, Speak et al. 2003, Pollack et al., 2008, Robertson et al., 2006) and TM charge creates noisy forces on the TM as charge and stray voltages fluctuate.
- *Electronics-related noise*: The back action of the injected sensing signals and noise in the actuation voltages create noisy electrostatic forces on the TM.
- *Optical radiation pressure*: The intensity noise of the laser beams bouncing off the test mass will generate technical radiation pressure noise.
- *Magnetic fluctuations*: Changes in the magnetic field around the TM will directly couple to any residual magnetic moment of the TM.
- *Gravitational fluctuations*: Changes in the mass distribution around the TM via thermal expansion or fuel tank depletion will change the gravitational force on the TM.
- *Stiffness*: Coupling between the housing and the TM, approximated as a negative spring, which converts any satellite jitter around the nominal TM position into force noise on the TM. Satellite jitter arises because of noise in the readout of the satellite-to-TM relative position, noise in the μN-thrusters used to position the satellite around the TM, and external disturbances such as time-varying atmospheric drag, albedo and solar radiation pressure.

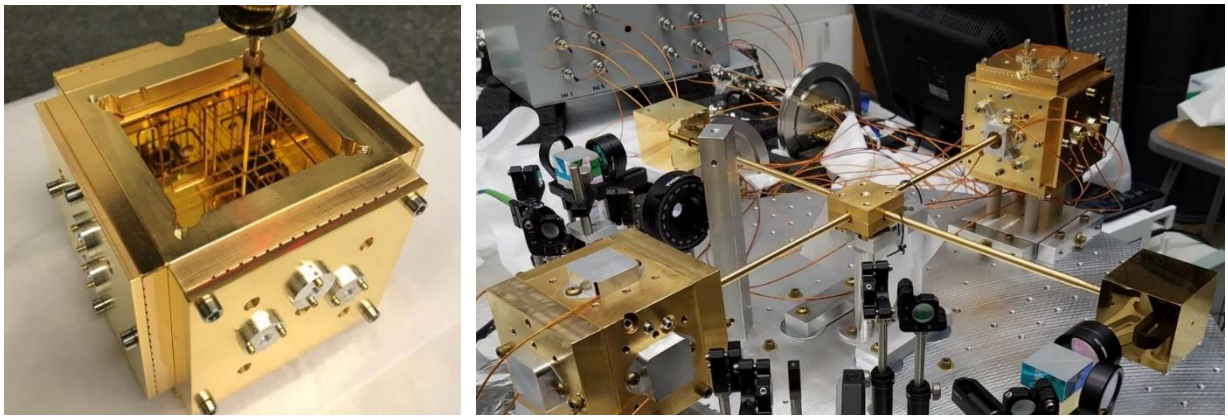

Figure 4. LISA Pathfinder equivalent gravitational reference sensor on the UF coordinate measuring machine (left) and integrated with the torsion pendulum and laser interferometer (top, right part of the right image)

rotational motion of the pendulum into translational motion of the test masses. The two test masses that are surrounded by inertial sensors are electrically isolated from the rest of the structure by quartz rings. This is needed for the bias injection scheme used by the capacitive readout. It also allows TM charge-related acceleration noise to be measured and for charge control to be demonstrated. The entire suspended structure is 0.5 kg and is coated with gold. The primary displacement readout for the pendulum is a polarization multiplexed Mach–Zehnder laser interferometer with a sensitivity of ~100 pm/Hz$^{1/2}$. The fundamental limit of the pendulum, shown in Figure 5, due to the fiber thermal noise is below 10^{-14} m/s^2 Hz$^{1/2}$ around 1 mHz, while the measured performance is ~4×10^{-13} m/s^2 Hz$^{1/2}$, consistent with the anticipated performance requirements for future Earth geodesy gravitational reference sensors.

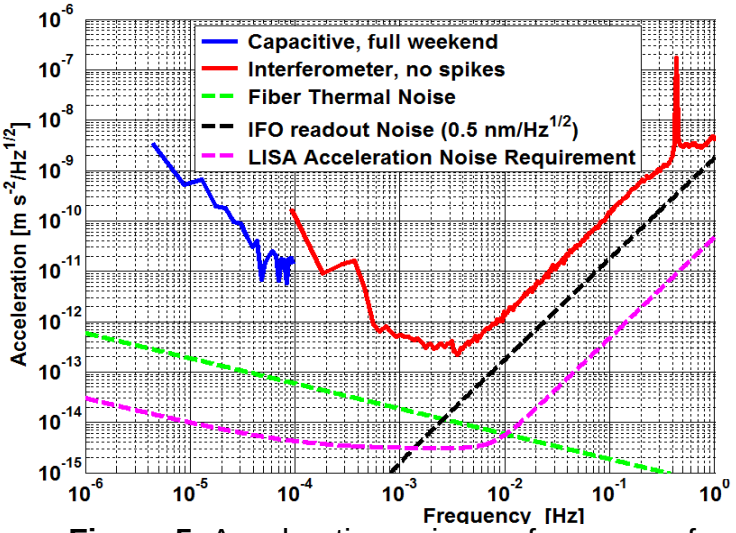

Figure 5. Acceleration noise performance of the UF torsion pendulum: <10^{-12} m/s^{2}Hz$^{1/2}$ over 0.5-10 mHz.

1.5 *Expected Acceleration Noise Improvement*

Based on the acceleration noise models discussed in the previous section and a spacecraft environment equivalent to that of GRACE-FO, the simplified GRS would have the acceleration noise performance shown in Figure 6(a) if operated on a drag-free platform and in Figure 6(b) if operated on a traditional spacecraft in a 500 km Earth orbit. Therefore, if the GRS were implemented on a GRACE-like mass change mission without drag-compensation we expect the performance to be that shown in Figure 6(b). However, if in the future the sensor were operated on a drag-compensated platform, it would have the performance shown in Figure 6(a). The spacecraft and drag environment models, based on flight data from GRACE-FO, are described in the next section. This sensor has an estimated acceleration noise that is 100 times lower (drag-free) and 10 times lower (non-drag-free at 500 km) than that of the GRACE accelerometers. The

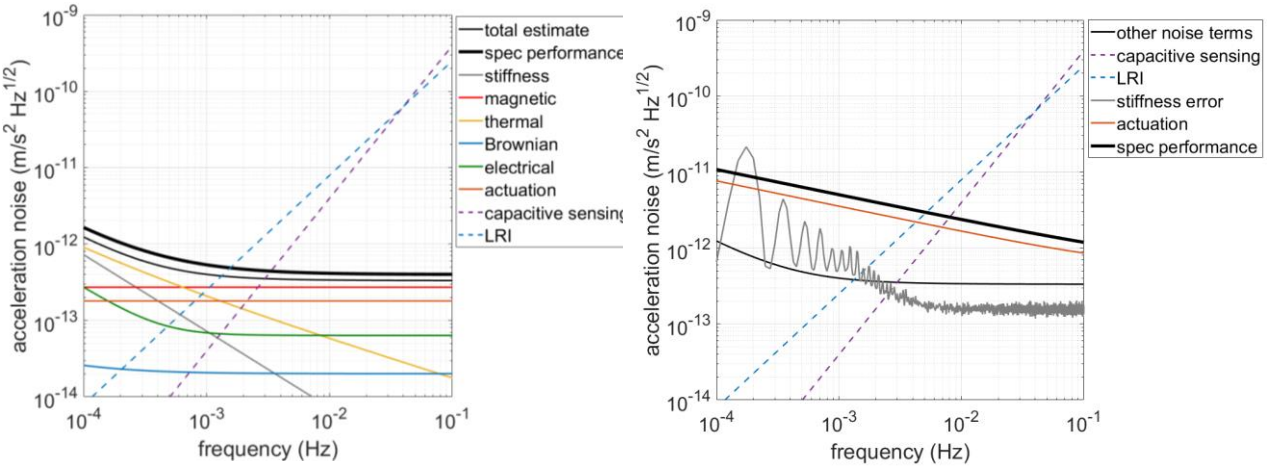

Figure 6. Acceleration noise model (estimate) for the simplified GRS, (a) operated on a drag-free platform and (b) operated on a GRACE-like spacecraft at 500 km, based on the measured GRACE-FO flight acceleration environment.

individual terms for the accelerometer noise model are grouped into seven categories: (1) stiffness, (2) magnetic, (3) thermal, (4) Brownian, (5) electrostatic, and (7) actuation (Gerardi, et al., 2014). Stiffness is the small residual coupling between spacecraft and TM motion. Brownian noise is mainly due to the residual gas inside the electrode housing, and electrostatic noise is mainly caused by the residual charge on the TM. In Figure 6(a), the total acceleration noise estimate is shown by the thin black curve, while the bold black curve represents the bounding performance given by Equation (1) below. In Figure 6(b), the total acceleration noise is equal to that shown in Figure 6(a) for a drag-free spacecraft (thin black curve) plus larger contributions from actuation noise (orange curve) and stiffness (grey curve). Note that the stiffness-induce noise was calculated using the measured spacecraft acceleration environment on GRACE-FO. Since actuation noise is dominating, the bounding acceleration noise curve (bold black curve) provided in Equation (2) below, is only based on this noise term. Also shown in Figures 6(a) and 6(b) are the displacement measurement noise curves for the LRI and GRS capacitive readout, doubly integrated to convert them to acceleration noise.

The following acceleration noise amplitude spectral densities, $S_a{}^{1/2}$, may be used to evaluate the gravity recovery capability of the simplified GRS over the frequency band of 0.1 mHz up to 0.1 Hz. These spectra bound the noise models and are also shown in Figure 6 as the bold, specified performance curves. For the drag-free model, the bounding acceleration noise amplitude spectral density (ASD) is:

$$S_a^{1/2} = 4 \times 10^{-13} \sqrt{1 + \left(\frac{700\ \mu\text{Hz}}{f}\right) + \left(\frac{300\ \mu\text{Hz}}{f}\right)^2}\ \frac{\text{m}}{s^2\ \text{Hz}^{1/2}} \qquad (1)$$

The white noise contribution is largely caused my magnetic effects, the $f^{-1/2}$ term by thermal fluctuations, and the f^{-1} term by stiffness-induced acceleration noise. If the simplified GRS were operated on a non-drag-free GRACE-like spacecraft in a 500 km Earth orbit, the acceleration ASD would be:

$$S_a^{1/2} = 5 \times 10^{-13} \sqrt{1 + \left(\frac{1\ \text{Hz}}{f}\right)^{2/3}}\ \frac{\text{m}}{s^2\ \text{Hz}^{1/2}} \qquad (2)$$

Here, the acceleration noise is dominated by noise from test mass actuation, which required to keep the TM centered in its housing.

By comparison, the acceleration noise of the GRACE-FO accelerometers is roughly 10^{-10} m/s^{2}Hz$^{1/2}$ around 1 mHz and 4×10^{-11} m/s^{2}Hz$^{1/2}$ at 100 mHz (Lebat et al., 2013). The performance is primarily limited by (a) measurement and actuation noise, (b) the thin (~10 μm) wire used for charge control which produces a $1/f^{1/2}$ thermal acceleration noise spectrum, and (c) electrostatic and other noise sources caused by the relatively small TM-to-housing gaps (175 μm). To achieve the improved performance of the simplified GRS we (a) use drag-free spacecraft reduce or eliminate the actuation noise, (b) we remove the small grounding wire and replace it with a UV photoemission-based charge control system, (c) we increase the mass of TM from 75 g to ~500 g, and (d) importantly, we increase TM-to-EH gap size to at least 1 mm. A larger gap size is made possible by the UV test mass charge control system that replaces the grounding wire. Using new UV LEDs to perform charge control will have little impact on the size, weight, and power of the instrument.

2 Relevant Mission Architectures and Key Spacecraft Interfaces

Like previous Earth geodesy missions (and space gravitational wave interferometers), instruments for Earth gravity field measurements include the entire spacecraft and its subsystems. The design of the payload is not easily separated from that of the spacecraft bus or the mission architecture. One must therefore consider not only the GRS but also the spacecraft platform and laser interferometer as a single "instrument". This includes the attitude control system, possible drag-compensation system and associated micropropulsion system, the thermal, electromagnetic, and gravitational environment, and the choice of constellation orbits. While evaluating and optimizing all relevant parameters for a candidate mission is outside the scope of this roadmap, we will discuss a few key properties of an ideal mission and spacecraft.

Table 1 shows the some of the key parameters used to estimate the acceleration noise amplitude spectral density shown in Figure 6. Many of these parameters describe the environment (thermal, electromagnetic, pressure) near the GRS and can therefore be considered interface requirements on the host spacecraft. Since the spacecraft environmental conditions and the design of the GRS are interdependent, several trade-offs between the spacecraft environmental requirements and the GRS design are possible for a given desired acceleration noise level. For example, the magnetic requirements are in part driven by the choice of TM material, and most of the environmental requirements can be relaxed if a more massive TM is used.

Most of the important spacecraft environmental parameters have already been provided in Table 1. *These parameters were based on the measured GRACE-FO spacecraft environment and assume only a modest level of magnetic shielding.* However, this level of thermal and electromagnetic stability are likely not consistent with a nanosatellite platform like a CubeSat. Microsatellite platforms, such as ESPA-class spacecraft, which have a mass that is roughly 1/3 of that of GRACE-FO may also be capable of providing such an environment for the GRS. The vacuum level should be achievable by venting the area around the GRS to space, like was done on LISA Pathfinder and on GRACE-FO for the laser stabilization cavity.

The acceleration noise model summarized in Figure 6(a) assumes a drag-free platform for the instrument. This is important for reducing or eliminating the electrostatic force needed to keep the TM centered in its housing, and more importantly, minimizing the associated electrostatic force noise on the TM. The most important performance metric for the drag-free system with respect to

TM acceleration noise is the spacecraft-to-test mass jitter. The acceleration noise model assumes 50 nm/Hz$^{1/2}$ at 1 mHz with a 1/*f* frequency dependence, which significantly higher than the capacitive readout sensitivity.

Table 1. The primary GRS and spacecraft environmental parameters used to produce the estimated acceleration noise of the GRS shown in Figure 6.

Quantity, variable		**Value**
TM mass, m		540 g
TM side dimension, s		30 mm
TM-EH gap, d		1 mm
EH mass, m_{EH}		1 kg
S/C mass, m_{SC}		500 kg
S/C-to-TM jitter, δx	Drag-free	50 nm/Hz$^{1/2}$ (1 mHz)
	Non-drag-free	2 μm/Hz$^{1/2}$ (orbital frequency)
Magnetic field at the TM, B		100 μT
Magnetic field fluctuation at the TM, δB		2 μT/Hz$^{1/2}$
Mag field gradient at the TM, ΔB		20 μT/m
Mag field gradient fluctuation at the TM, $\delta\Delta B$		0.5 μT/m Hz$^{1/2}$
Mean temperature at the TM, T		293 K
Fluctuations in temp change across EH, $\delta\Delta T$		5 mK/Hz$^{1/2}$ at 1 mHz
Spacecraft temperature fluctuations near the GRS, δT_{SC}		1 K/Hz$^{1/2}$ at 1 mHz
Pressure around the TM, P		10 μPa

The acceleration noise ASD provided in Figure 6(b) used the measured spacecraft acceleration time history as a direct input, in addition to the environmental parameters shown in Table 1 that were also based on the measured GRACE-FO environment. As previous stated, the force noise associated the test mass electrostatic actuation limits the performance of the GRS on a non-drag-free platform. The DC force authority of the actuation system was based on the measured DC atmospheric drag force acting on GRACE-FO at 500 km. At lower altitudes, the required DC actuation force on the TM would be higher and so would the actuation force noise. A simple model the test-mass actuation control scheme was used to compute the resulting spacecraft-to-test mass motion, which peaks at the orbital period with an amplitude of 2 μm/Hz$^{1/2}$. In the model shown in Figure 6(b), we assume that the stiffness coefficient can be measured and subtracted at the 5% level. LISA Pathfinder demonstrated stiffness calibration with percent-level accuracy.

The simplified GRS may be useful for many different mission architectures, including Low-low satellite-to-satellite tracking (LL-SST) missions, precision orbit determination (POD) missions, and gravity gradiometer missions. For POD missions, the GRS would be helpful for removing the orbit determination uncertainty associated with atmospheric drag and solar radiation pressure. For gravity gradiometer missions, multiple sets of GRS could be employed in a single spacecraft in a way that is similar to the GOCE mission.

The optimal and best understood architecture for the GRS would arguably be an LL-SST mission employing a laser ranging interferometer like GRACE-FO. Analysis of the performance of previous LL-SST missions, for example that which is summarized in Figure 1, indicate that a GRS would be valuable only if an LRI was used to measure the intersatellite range. The altitude of the two spacecraft is another key parameter that determines the gravity recovery quality. Lower altitudes require drag-compensation if a long mission lifetime is desired. Drag-compensation (or drag-free) is also required to achieve the specified performance of the GRS. Therefore, micropropulsion and drag-compensation would improve gravity recovery by *both* allowing lower altitudes *and* improving acceleration noise. It is important to note that thrust resolution and noise is mainly important for minimizing acceleration noise by minimizing spacecraft-to-TM jitter, while the maximum thrust requirement is mainly governed by the desired satellite altitude.

3 Heritage, Technology Readiness, and Risks

The heritage and technology readiness for the simplified GRS is different for each of its subsystems. It is important to note that the LISA Pathfinder GRS as designed and operated in the LISA Pathfinder mission exceeded all of its requirements and is therefore considered TRL 9. Work continues on the development of the GRS for the LISA mission, which is expected to operate in an Earth trailing orbit for ten years after a ~2.5 year cruise and commissioning phase. Since we are considering a simplified version operated on a different spacecraft platform in a different orbit, we consider the simplified GRS to be TRL 3-6. Table 2 is a summary of the TRL for the simplified GRS, with justification provided for each subsystem in the subsequent subsections.

Table 2. GRS TRL assessment summary.

GRS Subsystem	Current TRL	Future TRL with existing funding	Justification
EH and TM	3/4	3/4 (2021)	LISA GRS prototype integrated with the UF torsion pendulum
CMS	4	6 (2022 for LISA)	LISA CMS project at UF
FEE	3/4	3/4 (2021)	LISA FEE prototype using the in the UF torsion pendulum
CPM	2	3 (2021 via IIP grant at UF)	Will advance as part of existing IIP scope of work

3.1 *Test Mass and Electrode Housing*

A functioning prototype GRS electrode housing has been designed and constructed at the University of Florida. The EH is functionally equivalent to the LISA Pathfinder GRS EH and has an internal geometry and electrode layout that matches that of the Pathfinder GRS. The prototype unit and associated test mass are constructed from aluminum with ceramic electrode spacers, while the LISA Pathfinder EH is constructed from molybdenum with sapphire spacers and the test mass in constructed from an Au/Pt alloy. A photo of the prototype EH is shown in Figure 4. It is currently integrated with the UF torsion pendulum inside the pendulum's vacuum chamber and is undergoing performance testing. The simplified GRS electrode housing would be a scaled-down version of this prototype, with an internal cavity dimension of ~32 mm instead of the 54 mm cavity in the prototype LISA EH. Based on this work, the TM and EH are considered to be TRL 3-4 in the simplified and LISA geometries respectively and have a moderately low risk.

3.2 *Charge Management System*

The charge management system for LISA is a likely NASA contribution to the ESA-led mission and it is currently under development at the University of Florida. The flight hardware contribution is called the charge management device (CMD) and consists of the UV LEDs themselves, their fiber coupler and structural and thermal support, FPGA-based digital control electronics, an analog current source, and a fiber optic harness that delivers the UV light to the LISA GRS. This technology is currently funded by the NASA Astrophysics Division to reach TRL 6 by 2022 for the Class B LISA mission. The CMD for the simplified GRS would be identical, except have fewer channels. The LISA CMD contains 24 UV LED channels per spacecraft and supplies UV light to three different UV injection ports on two independent GRS. The simplified version would likely require just four cold-redundant UV LED channels to support a single UV injection port on the simplified GRS. We therefore consider the simplified CMD to be TRL 4 now, TRL 5 in early 2021, and TRL 6 before the end of 2022. Because the U.S. is leading the effort for the CMS for LISA, this subsystem for the simplified GRS is considered to be very low risk.

3.3 *Caging and Positioning System*

The CPM would require the largest amount of development effort to reach TRL 6. It is currently considered to be TRL 2, but will achieve TRL 3 by 2021 with existing funding through an IIP grant. The CPM is one of the higher risk elements of the simplified GRS. This is because none of the previously funded efforts in the U.S. were directed at developing a GRS caging system. One development path would be to replicate the CVM and GPRM used on LISA Pathfinder, since they operated successfully in that mission. However, the simplified GRS has a significantly lower TM mass than that of LISA Pathfinder and a greatly simplified CPM would be better optimized for this GRS.

3.4 *Electronics and Software*

The analog and digital electronics for TM sensing and actuation via the electrode housing, traditionally referred to as the Front-End electronics (FEE), have already undergone two design iterations at UF with sensing performance at the level of 5 nm/Hz$^{1/2}$ above 1 mHz for the simplified GRS. The GRS FEE is considered TRL 3 for the simplified sensor, but TRL 4 with the LISA-like sensor. Likewise, the digital control and analog current source for the charge management system are also quite mature, and will reach TRL 6 by 2022. The flight qualified FPGA used for the LISA CMS should have ample resources to handle both the CMS and the TM actuation and sensing functionalities. The only remaining development efforts for the electronics would then be for the CPM commanding and telemetry. Overall, the technical readiness of the simplified GRS electronics is TRL 3 and it is considered to be low risk technology.

4 Tasks Needed to Achieve TRL 6

The GRS development to TRL 6 would take advantage of previous NASA and European Space Agency investments in technology for Earth geodesy and space gravitational wave detection. The subsections below describe the tasks needed for three main GRS subsystems. We assume that the CMS being developed to the LISA mission requires little further development, and that only minor activities are needed to integrate the Front-End Electronics into the existing LISA CMS electronics and chassis.

4.1 *Test Mass and Electrode Housing*

The following tasks are deemed necessary to reach TRL 6 for the test mass and electrode housing. Excluded from these tasks is the work needed geometrically reference the electrode housing frame to the Laser Ranging Interferometer. We assume that, as a technology demonstration, the GRS would not be the primary inertial sensor on for the MCM. As such, the LRI triple mirror assembly (TMA) would reference the center of the primary inertial sensor. Therefore, a GRS mounting structure would need to be developed that geometrically links the TMA to the GRS electrode housing that is stable at the $nm/Hz^{1/2}$-level, which is equivalent to both the LRI and the GRS capacitive sensing capability. This effort is described in the LRI Technology Development Roadmap for MCM being written concurrently with this roadmap.

- **Year 1-2:** A prototype electrode housing and test mass will need be fabricated and tested. For TRL 4, the EH and TM could be fabricated from aluminum and ceramic following the same processes used to fabricate the prototype LISA-like GRS at the University of Florida. Even though the bulk material used to fabricate this TRL 4 prototype will not be representative of the flight unit, it will have the appropriate geometrical dimensions and surface coating, (Au), which is important for assessing the readout and actuation performance of the sensor. The actuation and capacitive sensing performance would be verified with respect to the requirements for the MCM with the smaller geometry of the simplified GRS. The acceleration noise performance would be verified via torsion pendulum experiments, for example by scaling the measured performance of the LISA-like GRS integrated with the UF torsion pendulum. Actuation performance would be verified via measured capacitance and measured applied voltages.
- **Year 2:** The TRL 5 EH and TM would be constructed from representative materials and have the representative form and function of the flight unit. The TRL 5 electrode housing should be designed to handle the expected launch environment and analyzed, for example by finite element analysis, to verify its structural performance. Vibration and shock testing could be performed on the unit integrated with the TRL 5 caging and positioning system as a risk reduction step before TRL 6 development. Its sensing and actuation performance would need to be verified with respect to requirements in the relevant environment for MCM in a thermal vacuum chamber. The magnetic susceptibility of the test mass would need to be measured to verify it is below the required level to keep magnetically-induced acceleration noise below the needed level. Completion of this work together with the previous task would constitute TRL 5 for the TM and EH.
- **Year 3-4:** We assume that industry will support TRL 4 and 5 development at a modest level with engineering services and safety and mission assurance. Starting at TRL 6, industry would take the lead on the fabrication and testing of hardware, including the electrode housing and test mass. The TRL 6 EH and TM would strive to be flight-like and would undergo comprehensive performance testing in the relevant environment using a thermal vacuum chamber. Shock and vibration testing would be performed on an integrated GRS head that incorporates the TM, EH, caging and positioning mechanism and the vacuum system. A new dedicated torsion pendulum would be used to verify the acceleration noise performance of the TRL 6 Electrode Housing.

4.2 *Front-End Electronics*

The Front-End Electronics provide the TM actuation voltage to the electrode housing and perform the capacitive readout of the TM position and orientation. We assume that the FEE would utilize the FPGA and power electronics already present in the LISA CMD which will reach TRL 6 by 2022.

- **Year 1:** The TRL 4 breadboard FEE would be a PCB populated with commercial off-the-shelf (COTS) parts, derived from the sensing and actuation electronics used in the UF torsion pendulum, but with the full functionality of the flight FEE. Its performance would be validated in a laboratory environment with respect to requirements. Capacitive sensing performance verified using TM & EH testbed described in Section 4.1. Actuation noise measurements and sensing performance can be verified at the FEE unit level through dedicated experiments to measure the generated actuation voltage noise and capacitive sensing performance. GRS system-level actuation and sensing performance requires the use of a precision torsion pendulum like the one at the University of Florida.
- **Year 2:** The TRL 5 version of the FEE would be populated with COTS components that have identified flight–equivalent parts. The design would take into account lessons learned from the TRL 4 development. It would be integrated into an electronics chassis that includes an FPGA controller, power electronics, as well as the electronics needed for the CMS and CPM. Its performance would be verified as in Year 1, in addition to testing in the relevant environment in a TVAC chamber. No shock and vibe at this stage, as CMS electronics unit would have already undergone these tests.
- **Year 3-4:** The TRL 6 FEE, would be an industry built flight-like unit and would use engineering units for flight EEE electronics components. It would be integrated into a CMD-like chassis with all of the electronics needed for the GRS, including FPGA controller electronics, power electronics, and other elements needed for the CMD and caging and positioning mechanism. The TLR 6 unit would undergo full functional and performance testing in the relevant environment and undergo complete environmental test (thermal, shock, vibration, and radiation).

4.3 *Caging and Positioning Mechanism and Vacuum System*

The following tasks are needed to achieve TRL 6 for the CPM and the GRS vacuum system. These tasks assume that mechanism selection and initial testing has occurred as part of the scope of the existing IIP grant.

- **Year 1:** During year 1, a breadboard version of the CPM based on the LISA Pathfinder GPRM and using the selected actuating mechanism would be designed and fabricated. The functionality of the unit would be tested in a laboratory environment. Models based on flight measurements from LISA Pathfinder and ground-based experiments for the LISA Pathfinder and LISA missions would be used to model adhesion forces and the "catapult effect" to predict the performance of the CPM in flight.
- **Year 2:** A higher fidelity CPM unit would be designed and fabricated from the chosen flight materials. Functional tests of the stand-alone unit would be performed before the unit is then integrated with the TRL 5 EH and TM. Environmental testing of the integrated unit would be performed, including shock and vibration with the test mass caged. Finally, the CPM would undergo repeated caging and release operations to verify the mechanism's lifetime with respect to the mission duration. We assume that mechanical caging of the test

mass may need to be performed several times in flight as part certain types of safemode operations.

- **Year 3-4:** The TRL 6 CPM would be an industry built, flight like unit integrated with the TRL 6 TM and EH, and controlled by the TRL electronics unit. It would undergo full performance and environmental testing, including those listed under Year 2.

4.4 *GRS Control Algorithms and Software*

In addition to test mass charge control functions, which is already being developed to TRL 6 for the LISA mission, the GRS software must also handle TM capacitive readout, electrostatic actuation algorithms and the feedback control laws associated with them, as well as caging and release operations and possibly safemode activities.

- **Year 1-2:** The TRL 4 software development effort would involve algorithm development and testing, focusing on TM sensing, actuation and control. The development would be driven my requirements for the MCM and use the required capacitive sensing noise levels, electrostatic actuation noise levels, the expected spacecraft acceleration environment, and thruster noise if a drag-compensation system is employed. TRL 5 development would integrate these algorithms into a complete firmware/software package that is written for the TRL 5 FPGA-based control electronics. Testing of the software would first be performed on numerical simulators for the full six degree-of-freedom GRS dynamics, then tested in one degree-of-freedom using a torsion pendulum with a LISA-like GRS. Results from this test would need to be scaled to the simplified GRS geometry.
- **Year 3-4:** Software development to TRL 6 would be led by industry and in addition to the functions listed above, it would incorporate standard practices for safety and mission assurance. This software/firmware would be implemented in the TRL 6 GRS and tested for functionality and performance using ground support equipment that incorporates numerical simulators for the GRS and spacecraft dynamics.

4.5 *Drag-Compensation System*

The GRS's acceleration noise performance is enhanced by a drag-free or a drag-compensation system. Such a system would eliminate or reduce electrostatic actuation forces on the TM, reducing the associated noise, as well as reducing the spacecraft-to-TM jitter, which contributes to stiffness-related acceleration noise. Drag compensation would also allow for lower altitudes, which improves measurement sensitivity. Here, we propose a set of tasks that would advance a drag-compensation system for the next Mass Change Mission that could be considered as an optional technology development effort beyond that of the GRS.

We assume that a micropropulsion system has been selected and a control system concept has been developed as part of the existing IIP grant scope of work. Given the wide range of high performance thrusters currently on the market and the experience from prior missions, including Earth Observing-1, LISA Pathfinder, Gravity Probe-B, GOCE, and Gaia, it is likely that a suitable, flight-ready micropropulsion system already exists. This application and architecture may require some additional testing to demonstrate meeting performance requirements (i.e. thrust noise), or if a higher performance is needed, then selection of system with a technology readiness of at least TRL 4 but preferably TRL 5 or TRL 6 is also possible.

If the drag-free or drag-compensation system were included in the next MCM as a technology demonstration, then it would likely need to function independently from the primary Attitude and Orbital Control Systems (AOCS). The drag-compensation system could include a higher thrust system, e.g. an ion thruster, for atmospheric drag compensation that works in tandem with a lower thrust but higher precision system that cancels fluctuations in the drag force (drag-free) and perhaps also performs spacecraft attitude control. The bang-bang AOCS on GRACE-FO imparts impulses on the spacecraft that adversely affects both the accelerometers and the LRI. A proportional attitude control thruster would mitigate these issues. Other functions of the heritage GRACE-FO AOCS may also be handled by the drag-compensation technology demonstration, including spacecraft despin/detumble activities, collision avoidance and orbit raising maneuvers.

- **Year 1-2:** Maximum thrust, thrust noise and resolution, and lifetime are the key performance requirements that must be met, with lifetime likely the driving requirement. One lesson learned from LISA Pathfinder is related to the difference in lifetime for the technology demonstration (LISA Pathfinder) versus the prime science mission (LISA). It is beneficial to develop thruster technology with the lifetime needed for the prime mission or at least develop a technology that is easily scalable, so that once the technology demonstration is completed, it is ready to be incorporated as a primary instrument in a follow-on mission. The first half of the technology development effort would involve either testing existing commercially available systems based on performance requirements or advancing the technology readiness of a higher-performance micropropulsion system. It would also include an assessment of thruster lifetime as well as development of the logic needed to perform the drag-free or drag-compensation control to TRL 5. This work would necessitate interaction between the thruster vendor and the GRS development team. The micropropulsion system would need to be tested in the relevant environment to demonstrate that is meets requirements. Note that prior to selecting the micropropulsion system and control strategy, it is challenging to cost the drag-compensation system technology development effort with confidence. Hence the wide range of costings.
- **Year 3-4:** The second two years would be an industry-led effort devoted to reaching TRL 6. A flight like propulsion system would need to be built and tested against the requirements in the relevant environment for the MCM, including shock, vibration, TVAC, and possibly radiation testing. The control system the handles drag-compensation and other functions described above would need to be developed, implemented in flight-like control electronics, integrated with the micropropulsion system, and tested in the relevant environment as well. The ground support equipment for this system would need to include a numerical simulator for the spacecraft dynamics and the disturbance environment in low Earth orbit.

5 Potential Future Advances and Other Applications

The acceleration noise performance of the simplified GRS can be improved further or relaxed by imposing stricter or more relaxed environmental requirements on the spacecraft. Mission simulation studies to date, however, indicate that acceleration noise below 3×10^{-13} m/s^{2}Hz$^{1/2}$ is likely not of value for LL-SST missions using intersatellite laser interferometry at the level of the GRACE-FO fundamental noise limit, which is governed by the LRI optical cavity thermal noise. Achieving acceleration noise performance better than a few$\times10^{-12}$ m/s^{2}Hz$^{1/2}$ on a drag-free spacecraft or a few$\times10^{-11}$ m/s^{2}Hz$^{1/2}$ on a traditional spacecraft with the currently used electrostatic

accelerometers is very challenging due to the dynamic range limitations of these sensors, the relatively small TM-to-EH gaps size used, the vacuum level achieved in the volume around the test mass, and the thermal noise associated with the TM grounding wire.

If the GRS was developed as a technology demonstration on the next MCM, it would likely be accommodated at a location away from the spacecraft center of mass, which would be occupied by the primary inertial sensor. It would also not be directly integrated with the LRI and would instead rely on a stable-enough structure to geometrically link the GRS housing to the LRI reference point. The LRI as a Prime Instrument Technology Development Roadmap includes tasks associated with developing this metrology structure, and as such we do not include them in this roadmap. If the technology demonstration were to be successful, then the GRS would be a likely candidate for the primary inertial sensor on a future Earth geodesy mission. In such a scenario, it would be advantageous to more tightly integrate the GRS and LRI. This could be achieved by re-locating the GRS to be at the center of mass of the spacecraft and directly integrating the LRI triple mirror assembly with the GRS housing. This would reduce systematic errors associated with spacecraft tilt-to-length coupling, reducing the measurement noise associated with spacecraft attitude motion. It would also reduce the volume and mass requirements for the combined inertial sensor and LRI.

Beyond the benefits associated with the next generation Earth geodesy missions, the development of GRS technology in the U.S. could also benefit future planetary science, fundamental physics, and gravitational wave missions. Precision gravity field mapping of Mars, for example, would improve our understanding of Martian geology and it's interior. Several proposed solar systems tests of general relativity also require precision drag-free sensors. Development of the simplified GRS in the early-mid 2020's would provide risk reduction for the ESA/NASA LISA mission because of the likely earlier timeline associated with the next Earth geodesy mission compared to LISA, which is expected to launch in the 2034 time-frame. It could also pave the way for a future NASA-led gravitational wave missions beyond LISA.

List of Acronyms

CBE, Current best estimate

CMS, Charge management system

CMD, Charge management device

CPM, Caging and positioning mechanism (on the simplified GRS)

CVM, Caging and venting mechanism (on LISA Pathfinder)

DMA, Drift-mode accelerometer

EH, Electrode housing

FEE, Font-end electronics

GPRM, Grabbing, positioning and release mechanism

GRS, Gravitational reference sensor

LL-SST, Low-low satellite-to-satellite tracking

LRI, Laser ranging interferometer

MCM, Mass Change Mission

POD, Precision orbit determination

SWaP, Size, weight and power

TM, Test mass

TMA, Triple mirror assembly

References

Antonucci, F., et al. (2011) LISA Pathfinder: mission and status, *Classical and Quantum Gravity*, Vol. 28, No. 1, 094001.

Armano, M., et al. (2018) Beyond the Required LISA Free-Fall Performance: New LISA Pathfinder Results down to 20 μHz, *Phys. Rev. Lett.*, Vol. 120, No. 6, 061101, doi: 10.1103/PhysRevLett.120.061101.

Bortoluzzi, D., Conklin, J.W., Zanoni, C. (2013) Prediction of the LISA-Pathfinder release mechanism in-flight performance, *Advances in Space Research*, Vol. 51, No. 7, 1145-1156.

Carbone, L., Cavalleri, A., Dolesi, R., Hoyle, C.D. Hueller, M., Vitale, S., Weber, W.J. (2005) Characterization of disturbance sources for LISA: torsion pendulum results, *Classical and Quantum Gravity*, Vol. 22, No. 10, S509-S519.

Carbone, L., Cavalleri, A., Ciani, G., Dolesi, R., Hueller, M., Tombolato, D., Vitale, S., Weber, W.J. (2007) Thermal gradient-induced forces on geodesic reference masses for LISA, *Physical Review D*, Vol. 76, No. 10, 102003.

Cavalleri, A., Ciani, G., Dolesi, R., Heptonstall, A., Hueller, M., Nicolodi, D., Rowan, S., Tombolato, D., Vitale, S., Wass, P.J., Weber, W.J., (2009) Increased Brownian Force Noise from Molecular Impacts in a Constrained Volume, *Physical Review Letters*, Vol. 103, No. 14, 140601.

Ciani, G., Aitken, M., Apple, S., Chilton, A., Olatunde, T., Mueller, G., Conklin, J.W. (2017) A New Torsion Pendulum for Gravitational Reference Sensor Technology Development, *Review of Scientific Instruments*, Vol. 88, No. 6, 064502.

Conklin, J.W. (2015) Drift mode accelerometry for spaceborne gravity measurements, Journal of Geodesy, Vol. 89, No. 11, 1053-1070.

Gerardi, D., Allen, G., Conklin, J.W., Sun, K-X., DeBra, D., Buchman S., Gath, P., Fichter, W., Byer, R.L., Johann, U. (2014) Invited Article: Advanced drag-free concepts for future space-based interferometers: acceleration noise performance, *Review of Scientific Instruments*, Vol. 85, No. 1, 011301.

Lebat, V., Boulanger, D., Christophe, B., Foulon, B., Liorzou, F., Perrot, E. (2013) Electrostatic accelerometer for the Gravity Recovery and Climate Experiment Follow-On Mission (GRACE-FO), *Fall AGU Meeting, San Francisco, CA, December 2013*.

Olatunde, T., Shelley, R., Chilton, A., Ciani, G., Mueller, G., Conklin, J.W. (2015) 240 nm UV LEDs for LISA test mass charge control, *Proceedings of the 10th International LISA Symposium, Journal of Physics: Conference Series*, Vol. 610, No. 1, 012034.

Pollack, S.E., Schlamminger, S., Gundlach, J.H. (2008) Temporal Extent of Surface Potentials between Closely Spaced Metals, *Physical Review Letters*, Vol. 101, No. 7, 071101.

Robertson, N.A., Blackwood, J.R., Buchman, S., Byer, R.L., Camp, J., Gill, D., Hanson, J., Williams, S., Zhou, P., (2006) Kelvin probe measurements: investigations of the patch effect with applications to ST-7 and LISA, *Classical and Quantum Gravity*, Vol. 23, No. 7, 2665.

Sheard, B.S., Heinzel, G., Danzmann, K., Shaddock, D.A., Klipstein, W.M., Folkner, W.M. (2012) Intersatellite laser ranging instrument for the GRACE follow-on mission, Journal of Geodesy, Vol. 86, No. 12, 1083-1095.

Speake, C.C., Trenkel, C. (2003) Forces between Conducting Surfaces due to Spatial Variations of Surface Potential, *Physical Review Letters*, Vol. 90, No. 16, 160403.

Wass, P.J. and the LISA Pathfinder Collaboration (2018) Precision charge control for isolated free-falling test masses: LISA pathfinder results, Physical Review D, Vol. 98 062001.